

1

2

Journal of Geophysical Research: Solid Earth

3

Supporting Information for

4

Strain accumulation and release rate in Canada: Implications for long-term crustal deformation and earthquake hazards

5

6

Adebayo Oluwaseun Ojo¹, Honn Kao^{1,2}, Yan Jiang^{1,2}, Michael Craymer³, and Joseph Henton³

7

8

¹Geological Survey of Canada, Natural Resources Canada, Sidney, British Columbia, Canada.

9

²School of Earth and Ocean Science, University of Victoria

10

³Canadian Geodetic Survey, Surveyor General Branch, Natural Resources Canada

11

12

Contents of this file

13

Figures S1 to S6

14

Tables S1 to S4

15

16

Additional Supporting Information (Files uploaded separately)

17

18

Table S1: The GNSS station horizontal velocities used in this study

19

Table S2: The compiled earthquake catalog used in this study

20

Table S3: The estimated moment rates at each grid in this study

21

Table S4: The estimated moment rates at actual seismic source zones used in the national seismic hazard model

22

23

24

Introduction

25

In this Supporting Information, we provide additional Figures (S1 – S6) to substantiate our results and discussion. Specifically, Figure S1 provides examples of the magnitude of completeness estimation using the maximum curvature method. Figure S2 presents examples of the distribution of geodetic moment rate and strain rate estimate for 6,000 bootstrap samples at grids located in relatively sparse and dense GNSS stations. Figure S3 presents the standard deviation of these distributions at each 2° x 2° grids. Figure S4 presents a comparison of the a and b-value estimate using the maximum likelihood method and least square regression. Figure S5 shows a map of the new estimate of seismic and geodetic moment rate at actual seismic source zones used in the 2015 national seismic hazard model.

34

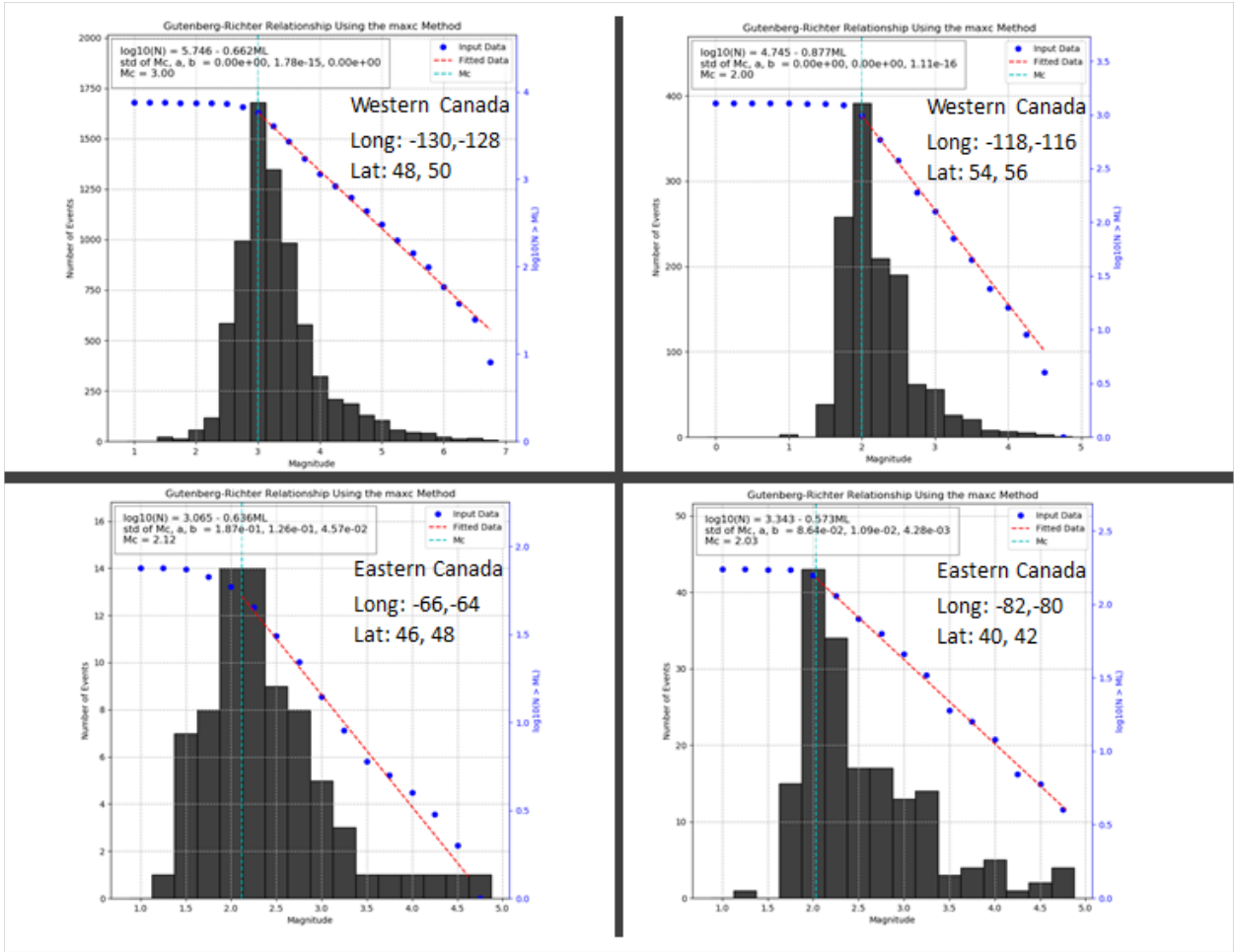
35 Lastly, Figure S6 shows the correlation between geodetic moment rate and the
36 number of events at each $2^\circ \times 2^\circ$ grid using different magnitude threshold.

37 Also, we present Tables S1-S4. Table S1 contains the estimated and compiled horizontal
38 velocities for GNSS stations included in this study. For each GNSS station, we provide the
39 geographical coordinates (longitude and latitude in degrees), the east and north velocities
40 (mm/yr), the associated uncertainties (mm/yr), and the time-span (years). We processed
41 RINEX data recorded by ~1000 Real-Time Kinematic (RTK) receivers across Canada using
42 the GIPSY v6.4 software package provided by the Jet Propulsion Laboratory (JPL).
43 Subsequently, we estimate the GNSS station velocities and associated uncertainties using
44 the robust Median Interannual Difference Adjusted for Skewness (MIDAS) software
45 available from the Nevada Geodetic Laboratory (NGL). We added more GNSS station
46 horizontal velocities from the JPL and the NGL online databases. Table S2 contains the
47 compiled catalog containing 45,114 earthquakes that occurred in western, central, and
48 eastern Canada in addition to the Northern part of the contiguous United States. We
49 provide information about the location of the event (longitude and latitude in degrees),
50 the estimated moment magnitude, and year of occurrence. Most of the data came from
51 the published 2011 Canadian Composite Seismicity Catalogue (Fereidoni et al., 2012). We
52 also include more recent earthquake records from the Composite Alberta Seismicity
53 Catalogue (CASC) which includes earthquakes in Alberta and northeastern British
54 Columbia (Fereidoni & Cui, 2015). Additionally, we include about 16,000 small magnitude
55 earthquakes ($M \leq 4$) contained in the Natural Resources Canada's (NRCan) online catalog
56 and the earthquake catalog of Visser et al. (2017) and estimate their moment magnitudes
57 following the Pseudo Spectral Acceleration (PSA) method of Atkinson et al. (2014). We
58 note that the uncertainty of the moment magnitude estimates for small events can be as
59 large as 0.5 magnitude units. Table S3 contains the main result from the computations
60 performed in this study. For each $2^\circ \times 2^\circ$ grid point, we provide the geographical
61 coordinates (longitude and latitude in degrees), the estimated geodetic moment rates
62 (Nm/yr) and their upper and lower bounds, the estimated seismic moment rates (Nm/yr)
63 and their upper and lower bounds from the moment summation method, the estimated
64 seismic moment rates (Nm/yr) and their upper and lower bounds from the truncated
65 Gutenberg-Richter (GR) distribution method. We input the term "N/A" to denote grid
66 points where no results were obtained for any of the moment-rates estimates. We note
67 that for sparse data regions, there is a possibility of obtaining more refined results in the
68 future with increasing density of broadband seismic stations and GNSS stations. Lastly,
69 Table S4 contains the results of estimated earthquake parameters, seismic and geodetic
70 moment rates at actual seismic source zones used in the 2015 national seismic hazard
71 model.

72

73

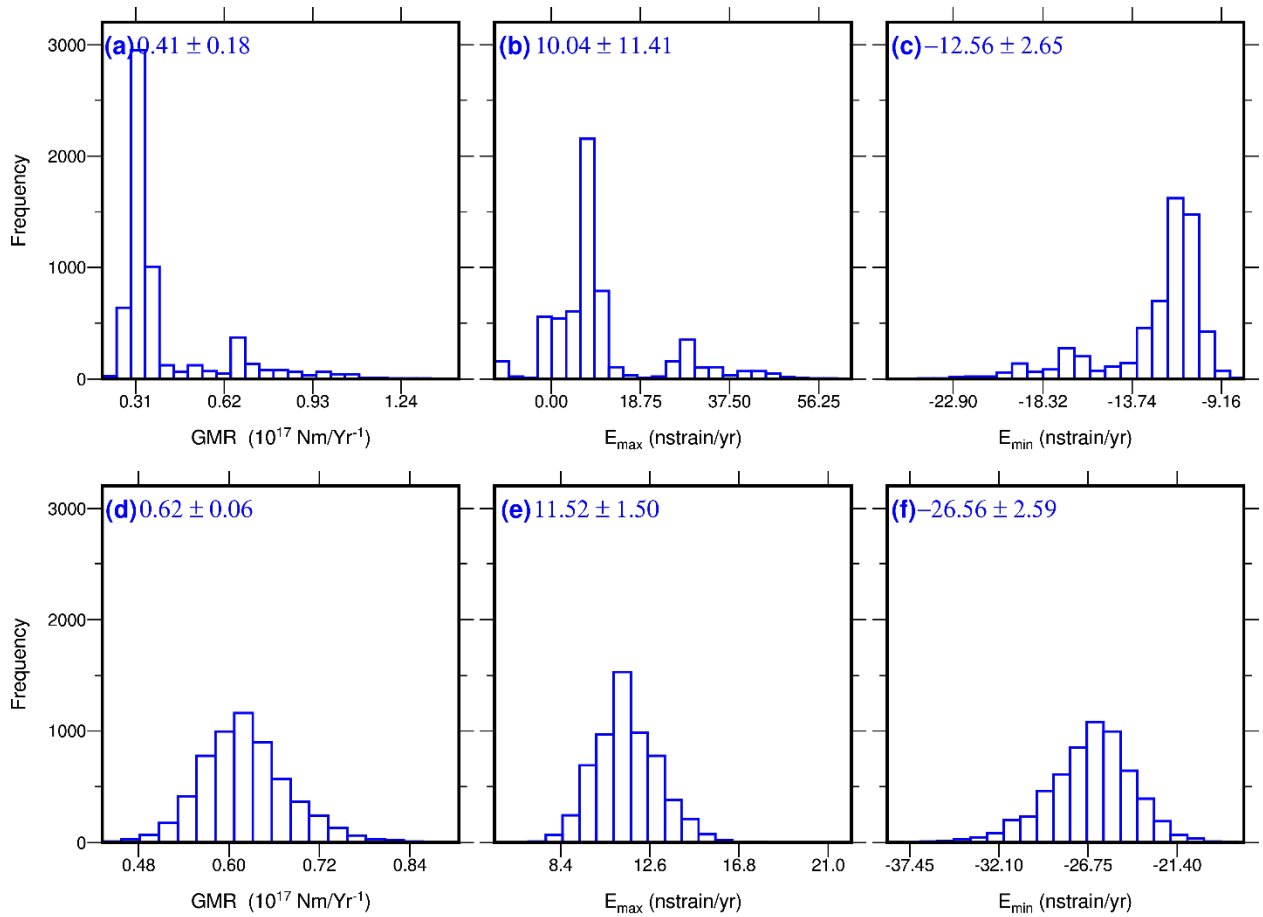
74



75
 76 Figure S1: M_c estimation using the maximum curvature method at four $2^\circ \times 2^\circ$ grids in
 77 western and eastern Canada. The black histograms are the frequency magnitude
 78 distribution of the earthquakes, the blue dots are the cumulative earthquake numbers, the
 79 red line is the best-fitted line from the G-R law, the green line denotes the curvature point
 80 which is the estimated M_c .

81

82



83

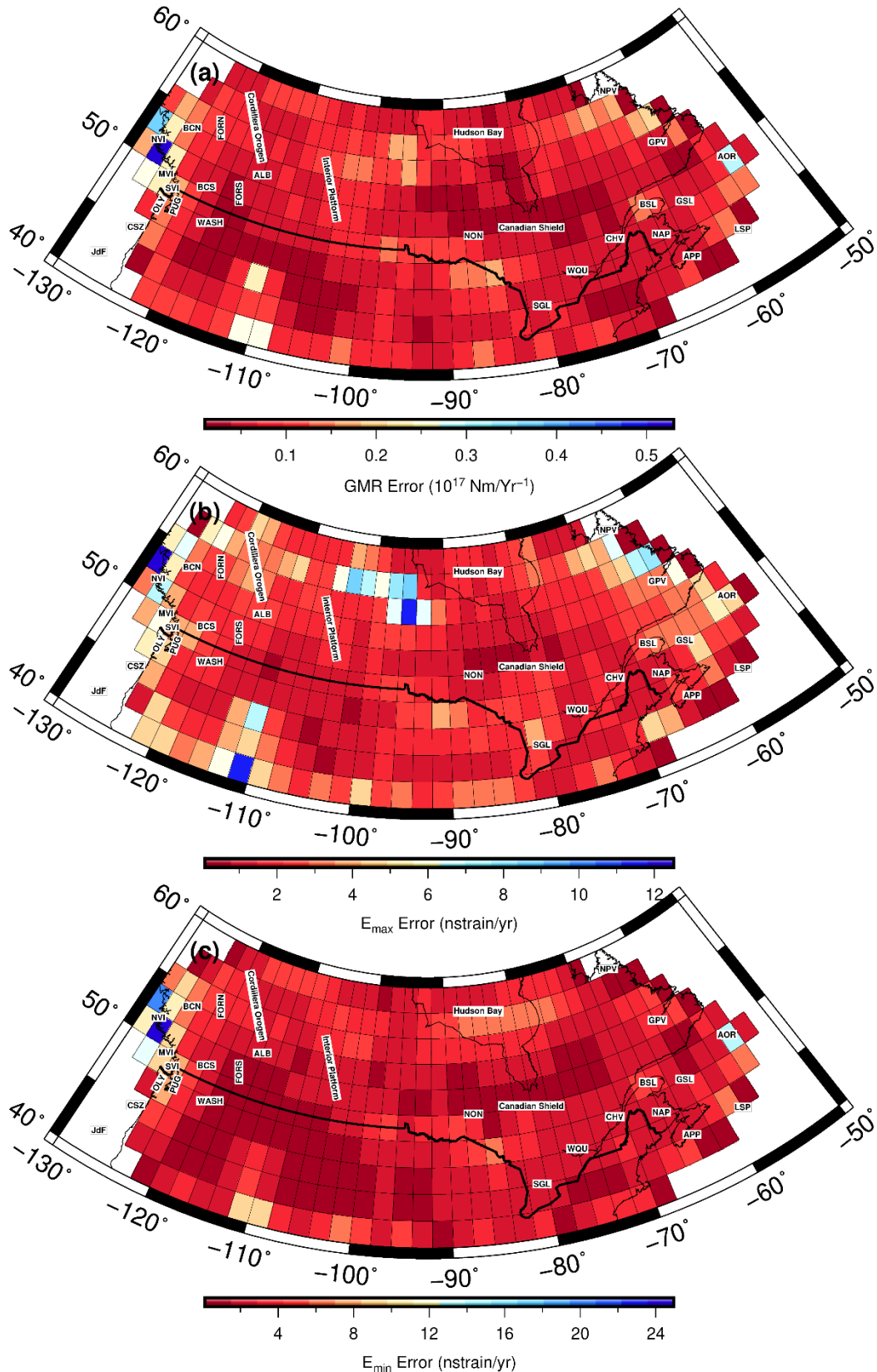
84

85 Figure S2: The distribution of parameters for 6,000 Monte Carlo simulations at two grid

86 points. (a, b, c) are geodetic moment rate, maximum, and minimum principal component

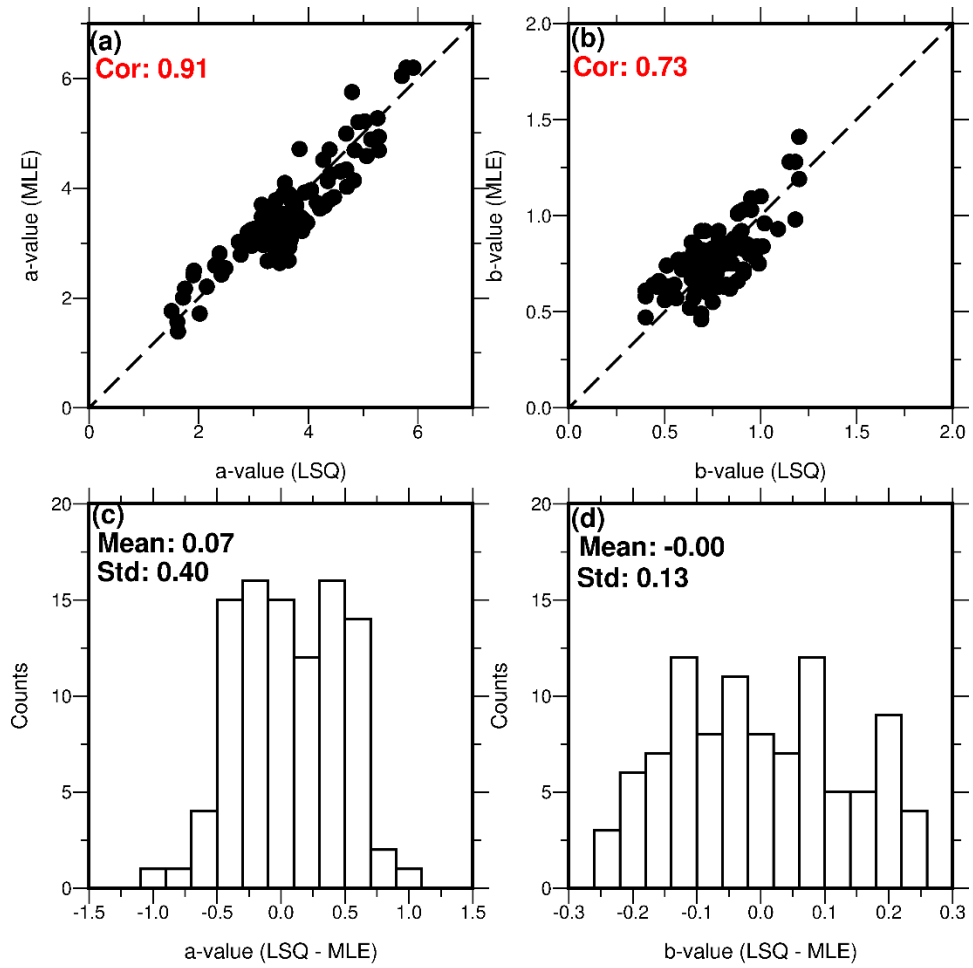
87 of the computed strain rate within a sparse GNSS station area in North-West Canada. (d,

88 e, f) is the same within a relatively dense GNSS station region in South-East Canada.



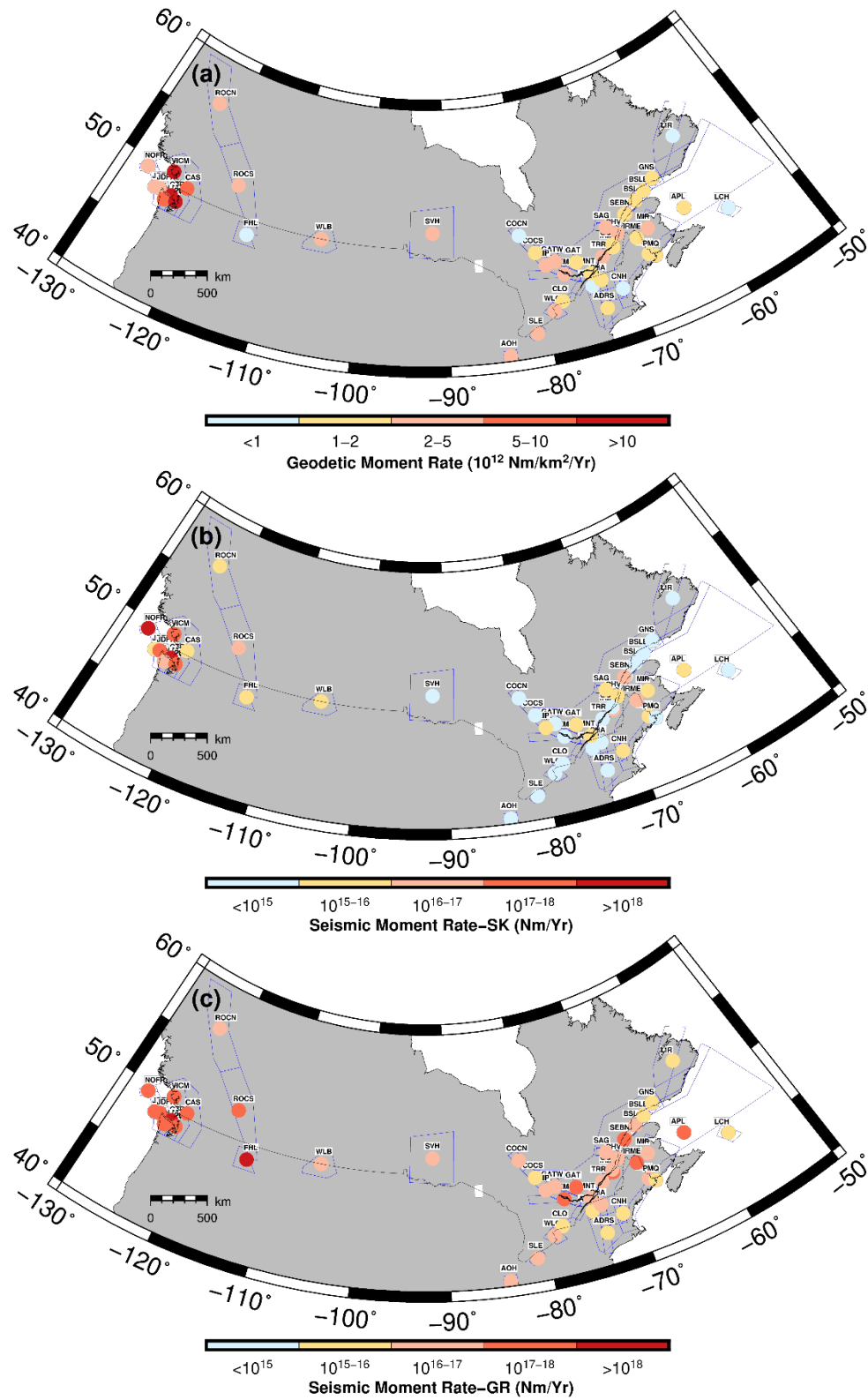
89
90
91

Figure S3: The standard deviation of the parameters from the 6,000 Monte Carlo Simulations at each $2^\circ \times 2^\circ$ grid point in the study area.



92
 93
 94
 95

Figure S4: Correlation between a and b-values from maximum likelihood (MLE) and least square (LSQ) methods.



96
 97 Figure S5: Estimated moment rates at exact seismic source zones used in the national
 98 seismic hazard model. (a) Geodetic moment rate normalized by source area (b) seismic
 99 moment rate from Kostrov equation (c) seismic moment rate from truncated G-R
 100 relationship.

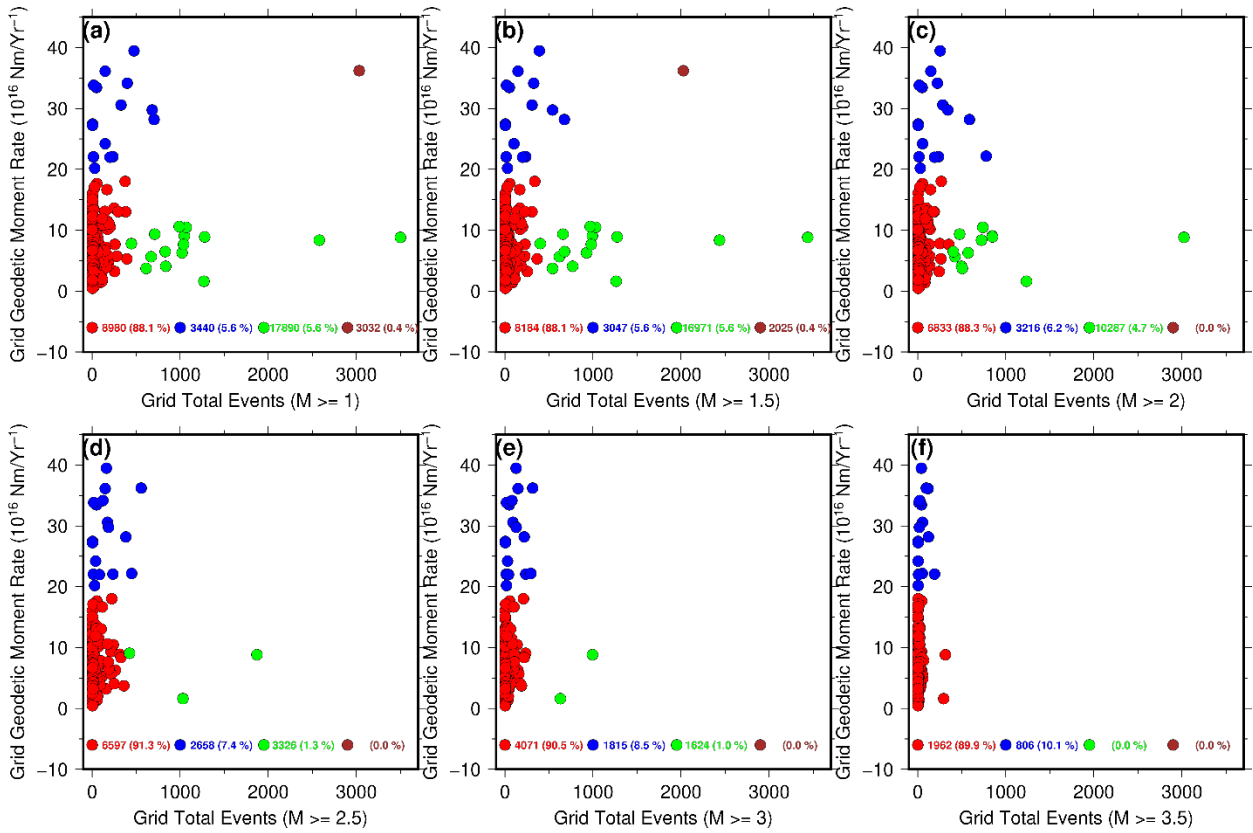


Figure S6: Relationship between the geodetic moment rate and the total number of events with varying magnitude threshold in each $2^\circ \times 2^\circ$ grid.

101
 102
 103
 104
 105
 106
 107
 108
 109
 110
 111
 112
 113
 114